Effect of Shrinkage Reducing Admixture on Time-dependent Pre-stress Losses in Pre-tensioned Beams

Salah Altoubat

Assistant Professor of Civil Engineering at the University of Sharjah, United Arab Emirates

ABSTRACT

Sixteen large scale pre-stressed concrete beams were tested under monotonic center point loading to determine the effect of shrinkage reducing admixture (SRA) on the time-dependent (TD) pre-stress losses in pre-tensioned beams. The nominal dimensions of the beam were 4.0 m x 0.20 m x 0.25 m (13 ft. 1.5 in. x 7.9 in. x 10 in.). The beams were reinforced with two straight, seven-wire, low relaxation strands of Grade 270. The SRA was added at dosage rates of 0%, 1% and 2%. The beams were instrumented and tested at variable ages ranging from 3 to 945 days. The flexural cracking load was measured and used to calculate the pre-stress force at the time of testing using principles of mechanics, and thus the pre-stress loss was evaluated at different ages. The results showed that the addition of SRA significantly reduced the pre-stress loss in the beams, particularly when added at 2%. The SRA reduced the TD pre-stress losses by up to 41.9 % and 37.6% at the ages of 735 and 945 days, respectively.

KEYWORDS: Pre-stressed concrete, Pre-stress loss, Shrinkage reducing admixtures, Shrinkage, Creep.

INTRODUCTION

Pre-stress losses have a direct impact on the concrete stress development and deflection behavior of pre-stressed concrete beams. It can be categorized as instantaneous loss and time-dependent (TD) loss. For pre-tensioned members, instantaneous losses are primarily due to elastic shortening of the beam, while time dependent losses are due to the shrinkage and creep of the concrete and the relaxation of the steel. Elastic shortening losses are easily determined by applying the pre-stressing force at the time of release to the beam section using mechanics of materials' approach. The time-dependent (TD) losses, however, are more complex, since they involve material properties and stress development, which all evolve

with time and are interrelated.

Shrinkage and creep of concrete are primary factors that drive the most significant TD losses in pre-stressed concrete. In view of the concrete microstructure, creep and shrinkage are not independent phenomena. They are interrelated and affected by a common process at the level of microstructure. The nature of the microstructure- and in particular the pore structure and the pore water- are key factors that have an influence on the shrinkage and creep of concrete. The low w/c ratio and high cement content generally used for pre-stressed concrete applications intensify the effect of shrinkage and creep on the pre-stress loss.

Using shrinkage reducing admixtures (SRA) is one of the methods to reduce the drying shrinkage of concrete. These water soluble liquids were developed originally in Japan (Nmai et al., 1998) and generally added to concrete at 1 or 2 percent by weight. The

mechanism of shrinkage reduction is attributed to a reduction of the surface free energy of the liquid/solid interface in a partially saturated pore structure, which then causes a reduction of the stresses generated by capillary tension during the drying process. Research on shrinkage of concrete with SRAs showed a reduction of the free shrinkage of lab specimens between 30% and 80% relative to the control specimens (Nmai et al., 1998; D'Ambrosia et al., 2001; D'Ambrosia, 2002; Folliard and Berke, 1997; Shah et al., 1997).

Some research studies have also shown that SRA reduced the tensile creep strain of concrete (D'Ambrosia et al., 2001; D'Ambrosia, 2002). Since SRAs affect the tensile creep of concrete, they will also affect the compressive creep because creep mechanisms in tension and in compression are similar in nature. Despite the significant reduction in shrinkage and creep of concrete with SRAs, the current models used in design codes for calculating creep and shrinkage are still lacking effective consideration of the SRAs. Recently, a modification to the GL 2000 model (Gardner and Zhao, 1993) taking SRAs into account was proposed by Al-Manaseer and Ristanovic (Al-Manaseer and Ristanovic, 2004), but the effects of SRAs on shrinkage and creep are still not incorporated in the majority of shrinkage and creep models available in the literature.

One potential application for SRAs is in pre-stressed concrete to reduce the TD losses associated with shrinkage and creep of the concrete. Pre-stress losses can be determined either numerically or experimentally. Numerical determination involves theoretical models to predict each component of loss of the pre-stressing forces. Several creep and shrinkage models are available to predict the creep and shrinkage behavior of concrete (ACI-209 (2001); CEB-FIP MC90 (1990); PCI Committee on Pre-stress Losses (1975); PCI Bridge Design Manual (1997); B3 (Baznat and Baweja, 1995); GL2000 (Gardner and Zhao, 1993); AASHTO LRFD (1998); Shams and Kahn (2000); and NCHRP Report 496 (Tadros et al., 2003). These models formed the basis for the existing methods to predict the TD losses in pre-stressed concrete such as the AASHTO Standard (1996);

AASHTO –LRFD (1998); the PCI Bridge Design Manual (PCI, 1997); and the NCHRP Report 496 (Tadros et al., 2003). These methods generally tend to over-estimate the TD losses associated with creep and shrinkage, in particular for high performance concrete as found by Christopher (2004). An over-estimate of pre-stress losses results in an overly conservative design for service load stresses and can also cause further design inefficiencies by limiting the span length of a girder, and by requiring a larger initial pre-stressing force to resist the applied loads, which, in turn, produces excessive camber. The over-estimate will be worse when an SRA is added to the concrete since none of the prediction methods account for the effect of SRA on the pre-stress loss. This may be partly attributed to the lack of theoretical models for creep and shrinkage of concrete with SRA and partly due to the lack of experimental data that demonstrate and quantify the effect of SRA on the pre-stress loss. The current study was intended to show the effect of SRA on the pre-stress loss in pre-tensioned beams through load testing of concrete beams fabricated for this purpose. Sixteen large-scale pre-tensioned beams were fabricated and tested at ages ranging from 3 days to 945 days. SRA was added to the concrete at 0%, 1% and 2% by weight of cement. The beams were tested in a three-point bending mode and the flexural cracking load was estimated. The effective pre-stress force at the time of testing was back-calculated using the principles of mechanics, and a trend on the time-dependent losses was established through testing the beams at various ages. The results are presented and discussed in this paper.

RESEARCH SIGNIFICANCE

SRAs significantly modify the shrinkage and creep behavior of concrete and thus will affect the time-dependent losses if they are used in pre-stressed concrete. Currently, the existing models, which provide an estimate of the losses, do not effectively account for the SRAs. This is due to a lack of creep and shrinkage models that account for the effect of SRAs and also due to the lack of experimental data that demonstrate the

effect of SRAs on pre-stress losses. A large-scale testing program was conducted on simply supported pre-tensioned concrete beams to study the effect of one particular SRA on the time-dependent pre-stress losses. The study contributes a set of sixteen large scale pre-

tensioned concrete beams with SRA to the existing literature. The test results will particularly be valuable to help calibrate existing models for pre-stress loss to take the effect of SRAs into account.
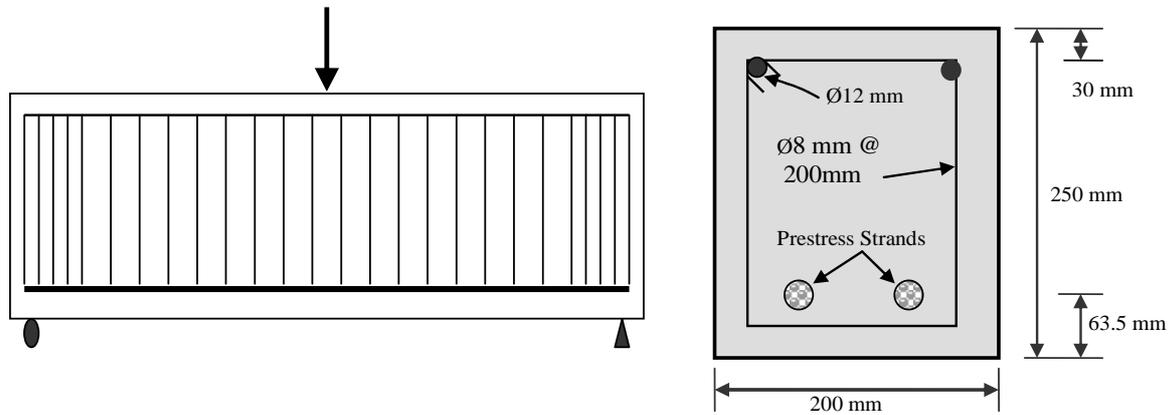
Figure 1: Details and cross-section of the beam

Figure 2: Fabrication of beams in the pre-stressing bed

EXPERIMENTAL PROGRAM

Experimental methods commonly used by researchers to determine pre-stress losses can be categorized into three major categories. The first category involves direct monitoring of the concrete strain inside the beam over time at the level of the center of gravity of the pre-stressing strands using embedded concrete strain gauges. This method has been proven effective and has been used by many

investigators to assess the pre-stress loss (Tadros et al., 2003; Yang and Myers, 2005; Stallings et al., 2003; Onyemelukwe et al., 2003; Gross and Burns, 1996; Labia et al., 1997). The second category involves load testing to determine flexural crack initiation and/or crack reopening loads and then back-calculating the effective pre-stress of the system using basic principles of mechanics. This method has also been used by many investigators (Labia et al., 1997; Pessiki et al., 1996; Halsey and Miller, 1996; Shenoy and Frantz, 1991;

Rabbat, 1984), particularly for girders removed from service or constructed for the sole purpose of testing. In this method, cracking loads were determined from visual observation of cracks or from strain and/or displacement measurements at the bottom of the beam. The third category is less common and involves exposing part of the strands and monitoring the strain of the strands upon cutting that portion by using strain gauges attached to the exposed strands. These methods have been used in many research studies and each has its limitations and drawbacks. These methods generally produce different results for the pre-stress loss even when used in the same girder as shown by Baran et al. (2005). The second approach was adopted in this study to evaluate the effective pre-stress in pre-tensioned beams at different ages.

Figure 3: Test setup and the arrangement of LVDTs

Large Beams' Testing Program

Sixteen large-scale pre-stressed concrete beams were designed, instrumented and tested in a displacement controlled mode under a monotonic three-point loading system in a simply supported configuration. The nominal dimensions of the beams were 4.0 m x 0.2 m x0.25 m (13 ft. 1.5 in. x 7.9 in. x 10 in.). The beams were reinforced with two straight 15.2 mm (0.6 in.) in diameter, seven-wire, low relaxation strands of Grade 270 placed in one layer at 51 mm (2 in.) from the bottoms of the beams. Two grade-60 steel bars with a diameter of 12 mm (0.47 in.) were added as compression steel at the top of the section to control possible cracking at transfer, and shear reinforcement of 8 mm (0.3 in.) closed-loop stirrups at 200 mm (7.9 in.) on center was incorporated in all beams. Spacing of the stirrups in the beam was reduced to 100 mm (4 in.) at the vicinity of the support points to improve confinement at these locations. Fig. 1 presents details and cross-section of the tested beam.

A hydraulic jack was used to tension the pre-stressing steel and each steel strand was initially loaded to a nominal tensile stress of 52% of its ultimate strength, which is equivalent to a jacking load of 135 kN (30.35 kips) per strand. The total pre-stressing force initially targeted for each beam was 270 kN (60.7 kips). The applied force is less than what the strands will normally be tensioned to in real structures, which can typically reach up to 75% of the ultimate strength of the strand. The stress ratio of 52% for the prestressing force was chosen to accommodate the testing capability of the lab. A similar stress ratio of 54% was also used in an experimental study of prestress loss by Baran et al. (2005). Moreover, the intent of this research project was to compare the time-dependent pre-stress loss of beams containing SRA with that of beams without SRA, and hence the targeted stress ratio of 52% was deemed appropriate and served the purpose.
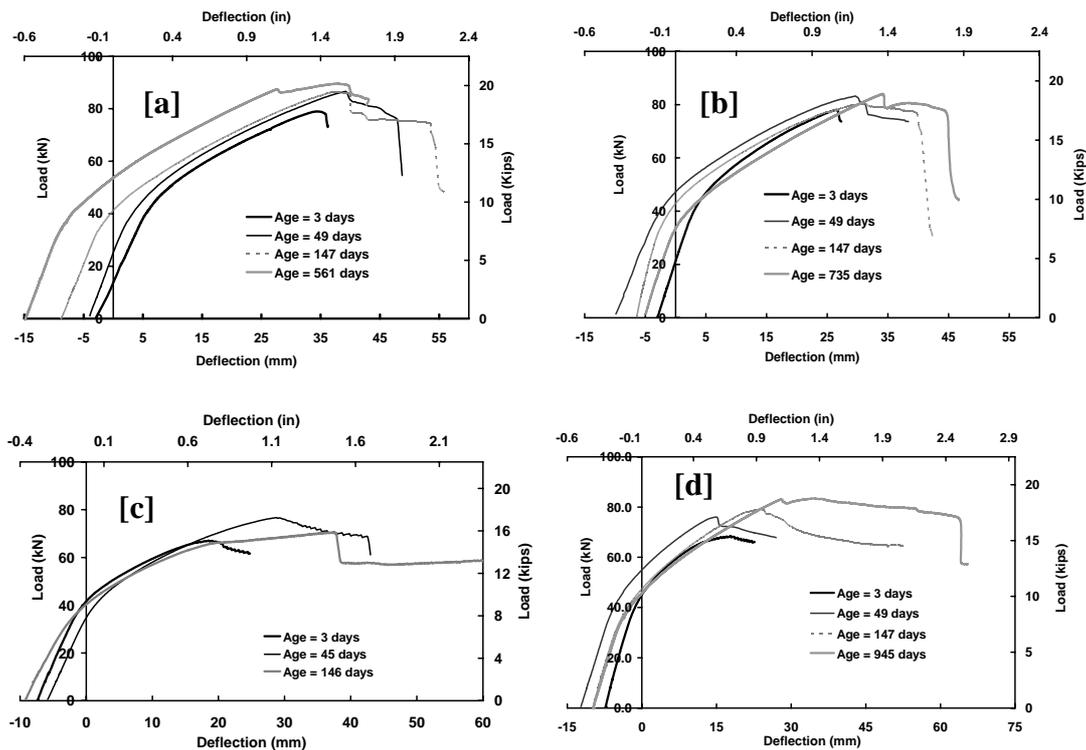
Figure 4: Load versus deflection curves of (a) control beams (b) beams with 1% SRA (c) beams with 2% SRA and (d) beams with 2% SRA and fibers

Formworks for two parallel rows of 8 beams were prepared in the pre-stressing bed of the precast plant (Fig. 2) and the strands and the steel reinforcement were installed in the beams. Two straight strands were installed in each row and the strands were jacked at one end to the required force. The use of single straight strands for the 8 beams with separators between the beams might induce some small variation in the pre-stressing force for individual beams. However, this variation may not be critical given that the strands were all straight. The total number of beams was 16 divided into four sets (each set consisted of 4 beams). The first set of beams was made out of plain concrete without SRA (control beams); the second set of beams was made out of concrete with 1% SRA by weight of cement; the third set of beams was made out of concrete

with 2% SRA; and the last set of beams consisted of concrete beams with 2% SRA and 0.5% by volume of concrete of synthetic macro-fibers. The use of fibers in the last group was intended to show whether the fibers can have an effect on the pre-stress losses or not and also served as a duplicate for the third set of beams since it contained 2% of SRA, which is the most effective dosage rate of SRA according to the supplier's data sheet. Two Ready Mix Concrete (RMC) trucks were needed to deliver the concrete volume to cast the beams. The first truck was used to cast the concrete beams without SRA (control) and the beams with 1 % of SRA after adding the admixture to the remaining concrete. The second truck was used to cast the remaining two sets of beams with 2% SRA.

Concrete cubes (150mm x 150mm x 150mm (6in. x

6in. x 6in.)) for compressive strength measurements and concrete prisms (75mm x 75mm x 285mm (3in. x 3in. x 11.25in.)) to measure the free shrinkage of the concrete were also cast for each set. The beams and other test specimens were steam-cured for 24 hours, and the

strands were cut off after the concrete gained sufficient strength. The beams and the test specimens were then transferred to the structural lab and stored inside the lab at room temperature until the time of testing.

Table 1: Mix proportions of the concrete mixtures

Materials	SRA= 0.0%	SRA= 1.0%	SRA= 2.0%	SRA=2.0% & fibers
Coarse Aggregate (20 mm), kg/m^3	750	750	750	750
Coarse Aggregate (10 mm), kg/m^3	320	320	320	320
Crushed Aggregate (5 mm), kg/m^3	305	305	305	305
Natural Sand, kg/m^3	305	305	305	305
Dune Sand kg/m^3	210	210	210	210
Cement, kg/m^3	400	400	400	400
Water, kg/m^3	148	148	148	148
Superplasticizer P25 MBT, Lit./ m^3	1.25	1.25	1.25	1.25
Superplasticizer RH857 MBT, Lit./ m^3	6.5	6.5	6.5	6.5
SRA Eclipse Lit./ m^3	0	4.28	8.57	8.57
Fibers (STRUX 85/50) kg/m^3	0	0	0	4.6
Water to Cement Ratio	0.37	0.37	0.37	0.37

1 kg/m^3 = 1.686 lbs/yd^3; 25.4 mm = 1 inch

Table 2: Compressive strength of concrete (MPa)

Age	SRA= 0.0%	SRA= 1.0%	SRA= 2.0%	Fibers& SRA=2.0%
12 hrs*	35.5	37.0	29.5	30.5
18 hrs*	44.5	46.0	30.0	33.5
3 days	48	47	35	38
49 days	59.5	54.6	46.6	51.6
148 days	60.2	58.3	56.1	55.1
561 days	60.4	-	-	-
735 days	-	60.3	59.2	58.4

* Concrete was under steam curing; 1 MPa = 145 psi

Material Properties

High strength concrete with a target compressive strength of 50 MPa (7250 psi) was used. The design water to cement ratio was 0.37. Crushed aggregates with aggregate sizes of 20 mm (0.8 in.) and 10 mm (0.4 in.) were used. The fine aggregate constituents were crushed aggregate with a maximum size of 5 mm (0.2 in.),

natural washed sand and dune sand. The mix proportions of the concrete used for casting the beams are presented in Table 1. The final water to cement ratio was around 0.37. The coarse to fine aggregate ratio was targeted at 56:44. A glycol-based shrinkage reducing admixture (SRA) sold under the brand name Eclipse® was added to the concrete at different dosages; 0%, 1% and 2%.

Table 3: Loads corresponding to flexural cracking and ultimate capacity of the beams

Beam Type	Age (days)	Flexural Cracking Load, kN	Ultimate load, kN	Modulus of Rupture (MPa)
Control Beams	3	38	79	5.19
	49	34	86.6	5.99
	147	33.5	86.5	6.14
	561	31.5	89.5	6.05
SRA = 1 %	3	37.5	78.1	5.12
	49	33.5	83.3	5.66
	147	33	80.4	5.98
	735	32	84.0	6.04
SRA = 2 %	3	35	67.1	4.21
	48	34.5	76.7	5.08
	149	33.5	70.6	5.89
	738	34	82.1	5.97
SRA = 2% & fibers	3	36	68.5	4.44
	49	35	76.1	5.40
	149	34.5	79.1	5.68
	945	34	83.5	5.9

1 kN = 224.809 lbf ; 1 MPa = 145 psi

Table 4: Effective pre-stress force and percentage difference relative to control

Age (days)	Control	SRA = 1%		SRA = 2%		SRA = 2% & fibers	
	Pre-stress force (kN)	Prestress force(kN)	% Increase	Pre-stress force (kN)	% Increase	Prestress force (kN)	% Increase
3	266.1	263.0	-1.16	258.4	-2.89	262.8	-1.24
49	213.1	215.3	1.03	236.1	10.8	234.1	9.9
148	205.6	204.2	-0.68	210.6	2.43	223.9	8.90
735	188.9*	193.6	2.49	213.5	>13.02	214.6**	>13.61

* this value was for the beam at the age of 561 days; 1 kN = 224.809 lbf.
** this value was for the beam at 945 days.

The main components of the polymeric fiber used (STRUX® 85/50) for the fiber reinforced concrete mixture are polypropylene and polyethylene. The fiber's nominal length is 50 mm (2.0 in.) with an aspect ratio of 85 and a specific gravity of approximately 0.92. The average tensile strength of the fiber is 540 MPa (78 ksi) with a modulus of elasticity of 9500 MPa (1380 ksi). The fibers were added to the concrete at a volume fraction of 0.50 %, which corresponds to 4.6 kg/m³ (7.75 lbs/yd³).

The cube compressive strength for the four concrete mixtures was measured at different ages according to BS 1881. The compressive strength measurement started 12 hours after casting and continued as testing of the beams progressed. The results are summarized in Table 2. As can be seen from the results, the compressive strength varied partly because of the addition of the SRA, particularly at a dosage rate of 2%. The compressive strengths of the control mix and the mixture with 1% SRA were comparable as well as the

strength development over time. The mixture with 2% of SRA showed lower early strength than the control set and the strength development was also lower. The compressive strength due to the addition of 2% of SRA was 30 MPa compared to 45 MPa for control mix at the age of 18 hrs, and 35 MPa compared to 48 MPa for control at 3 days, indicating that the cement hydration was slowed down. However, the concrete mix with 2% SRA recovered its strength as time passed on and became comparable to the control after six months as can be inferred from the results in Table 2. Many researchers have reported a loss of strength of up to 10% with the addition of SRA (Shah et al., 1992; Berke et al., 1997). The manufacturer's recommendations call for a reduction of the w/c ratio to offset the liquid content of SRA to achieve consistent workability, which may offset any loss of strength. However, this recommendation was not adopted in this project and thus a lower compressive strength was measured at early age. Another factor that perhaps contributed to this reduction of strength was the use of two different concrete trucks for casting the beams.

Table 5: Percentage reduction in total and time dependent losses due to the addition of SRA

Age (days)	% Reduction in Total Pre-stress Losses			% Reduction in Time Dependent Losses		
	1% SRA	2% SRA	2% SRA & fibers	1% SRA	2% SRA	2% SRA & fibers
3	-	-	-	-	-	-
49	3.96	40.3	37.0	10.0	57.9	45.9
148	-2.1	7.74	28.5	3.31	21.0	35.8
735	5.8	30.3	-	10.2	41.9	-
945	-	-	31.7	-	-	37.6
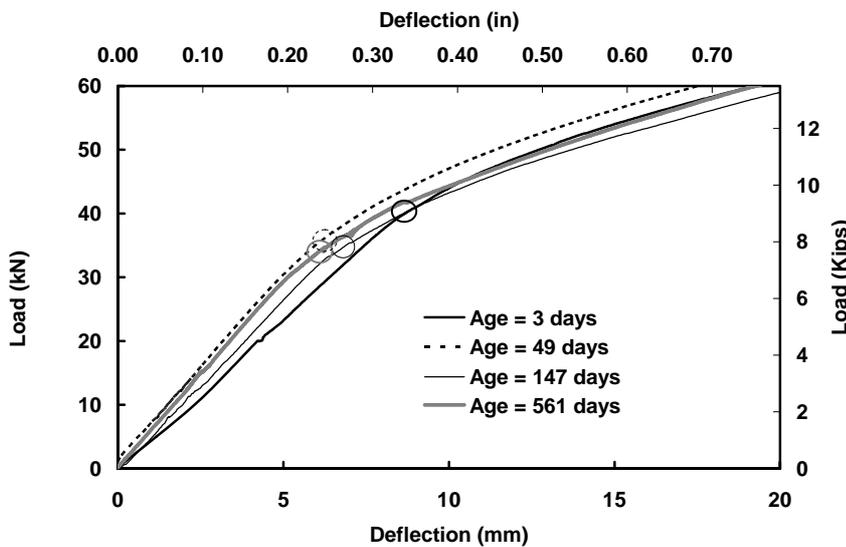
Figure 5: Closer look at the load deflection curves for control beams

Despite the fact that the target compressive strength was reached in time, the reduction in early strength caused by the addition of 2% SRA influenced the elastic losses, particularly at the time of transfer due to beam shortening. This complicated the analysis of the total pre-stress losses. However, and since the objective of

this research was to determine the time-dependent stress losses, the variability of the early strength of the concrete put the SRA beams at a disadvantage compared to the control beams with regard to the creep behavior. Creep of concrete generally tends to increase as concrete strength decreases. Consequently, the results

obtained in this research will form a lower bound for the effect of SRA on the time-dependent prestress losses for these particular beams tested in this study. The performance of the concrete beams with SRA in terms of TD losses would have been better if the early strength was comparable to the control mix.
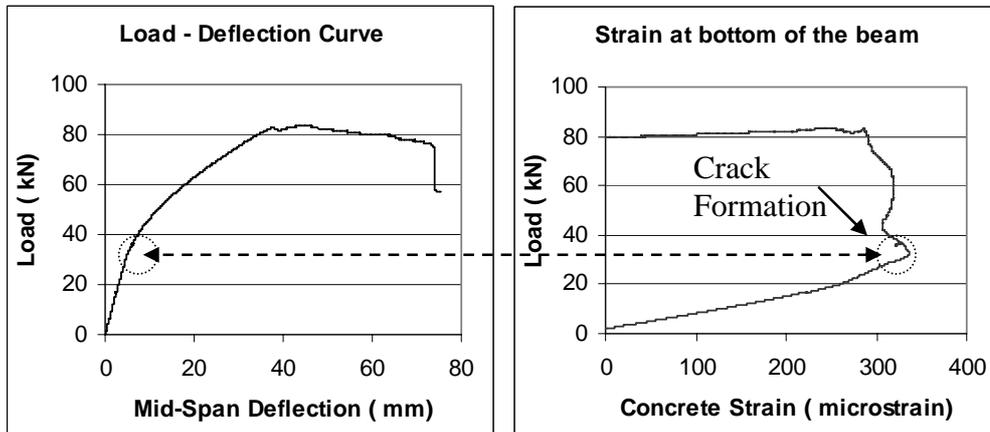
Figure 6: Strain and deflection response of the beam at cracking
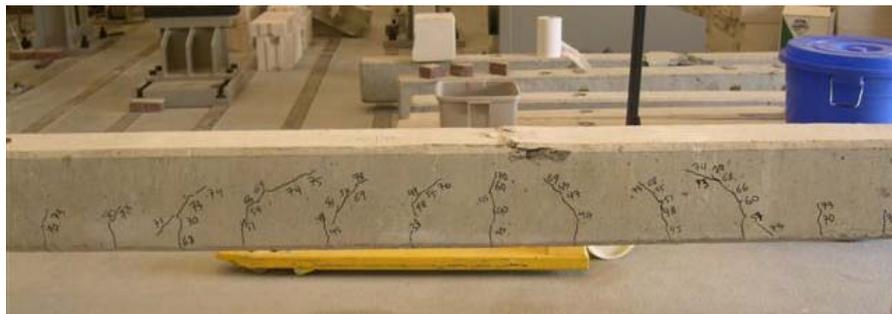
Figure 7: Typical cracking pattern in the tested beams

Testing and Measurements

The beams were tested in three-points bending using a 100 kN (22.5 kips) hydraulic actuator as shown in Fig. 3. The test setup consisted of a simply supported loading configuration with roller supports to prevent restraint to axial elongation. The load was applied onto the beams at mid-span (center point) and the test was performed in displacement control mode at a constant rate of 1.8 mm/min (0.07 in./min).

The four sets of beams were labeled and stored under the same environmental conditions in the lab

(room temperature and relative humidity of 50%). The four beams of each set were labeled as A, B, C and D. The first testing series was conducted with beam A of each group at the age of three days. These test results were aimed to establish a benchmark for the analysis of the time dependent prestress losses. The subsequent testing of two sets of beams was conducted at the ages of 49 days and 148 days. The last set was tested after a long drying period and conducted at the age of 561 days for control beams; 735 days for the beams with 1% and 2% of SRA; and 945 days (almost 3 years) for the

beams with 2 % SRA and fibers. At each age, one beam from each set was tested.

The parameters measured during the monotonic testing were: beam deflections, strain in the concrete, flexural cracking load and maximum load. The deflection of the beams at mid-span was measured with two linear voltage displacement transformers (LVDTs) with a range of ± 50 mm (± 2 in.). Some of the beams were also instrumented with concrete strain gauges attached to the bottom surface of the beam at mid-span to help evaluating the first flexural cracking load and validating its estimation process. Cracking pattern and sequence were also monitored during the load testing. Results from the strain and deflection measurements were used to explain the overall structural response of the beams and to estimate the pre-stressing force at the time of testing. The load levels corresponding to the beam's flexural cracking strength as well as the ultimate capacity were determined using visual observation and interpretation of the beam deflection and strain data. The formation of the first visually observed flexural crack was associated with a clear deviation from linearity in the load versus deflection curve and a sudden change of the concrete strain at the bottom of the beam. The load corresponding to the point at which the load deflection curve changes from linear to nonlinear behavior was found to be a good estimate of the flexural cracking strength. This load was used to back calculate the net pre-stressing force in the beam using basic principles of mechanics. The maximum load carried by the beam marked its ultimate flexural capacity. Furthermore, the camber of the beams was monitored over time and the variation was also used to assess the effect of the SRA on the time-dependent deformation of the beam.

EXPERIMENTAL RESULTS AND DISCUSSION
Load-Deflection Results

The load versus mid-span deflection curves of the beams tested from all four sets are presented in Fig. 4a - d. Each figure shows the load versus deflection curves of beams from the same set tested at different ages. The load versus deflection response was similar for all beams. It was linear up to the point of flexural cracking, after which the response became clearly non-linear but increasing until the maximum load carrying capacity was reached. The results show an increasing trend of the beam's ultimate strength with time for all sets, which was mainly attributed to the increase of concrete compressive strength, particularly that the time-dependent prestress losses did not affect the ultimate strength of the beam. The flexural cracking load (load at which flexural crack formed) was associated with a sudden change of the beam's stiffness and the load-deflection response change from linear to non-linear behavior. This point in the load deflection curve of the pre-stressed concrete beam is directly related to the net pre-stressing force and thus its estimate was essential. The load deflection curves indicate that the cracking load decreased with the age of the beam and this can be clearly seen through a closer look at the load deflection curves as shown in Fig. 5. Careful examination of the load deflection curves presented in Fig. 4a - d further reveal that the most decrease in cracking load occurred in the control beam and the least was seen in the concrete beams with 2% SRA. This decrease of the cracking load with time suggests that the pre-stressing force was decreasing due to the time dependent losses associated with shrinkage and creep of the concrete.

Another important characteristic of the beam deflection behavior is related to the beam camber (deflection due to prestress force (initial deflection in the load deflection curves)) after transfer and the change of it over time. Fig. 4a and b show that the amount of camber at the age of 3 days was similar for the control beam and for the beam with 1% of SRA. The control beam, however, exhibited a significant increase of camber with time as can be clearly seen in Fig. 4a whereas it increased to a lesser extent for the beam with 1% SRA as shown in Fig. 4b. The change in the beam camber is caused by the time-dependent deformation of the concrete beam, which is indirectly associated with the loss of the pre-stressing force. The results in Fig. 4a and b suggest that the loss was bigger for the control beams relative to the beams with SRA. For the beams

with 2% SRA (Fig. 4c), the amount of camber at the age of 3 days was greater than that of the control beam, and this was mainly attributed to the lower concrete strength of the beam with 2% SRA relative to the control beam at the time of transfer as mentioned earlier. This suggests that the camber right after transfer was greater due to the lower stiffness of the SRA beam. It also implies that the instantaneous loss due to elastic

shortening was greater in the beam with 2% SRA. The change of camber with time for the beams with 2% SRA (Fig. 4c and d) was less than the corresponding change of the control beams. This suggests that the loss in pre-stressing force due to time-dependent deformation of the concrete (shrinkage and creep) was smaller when the SRA was added at 2%.
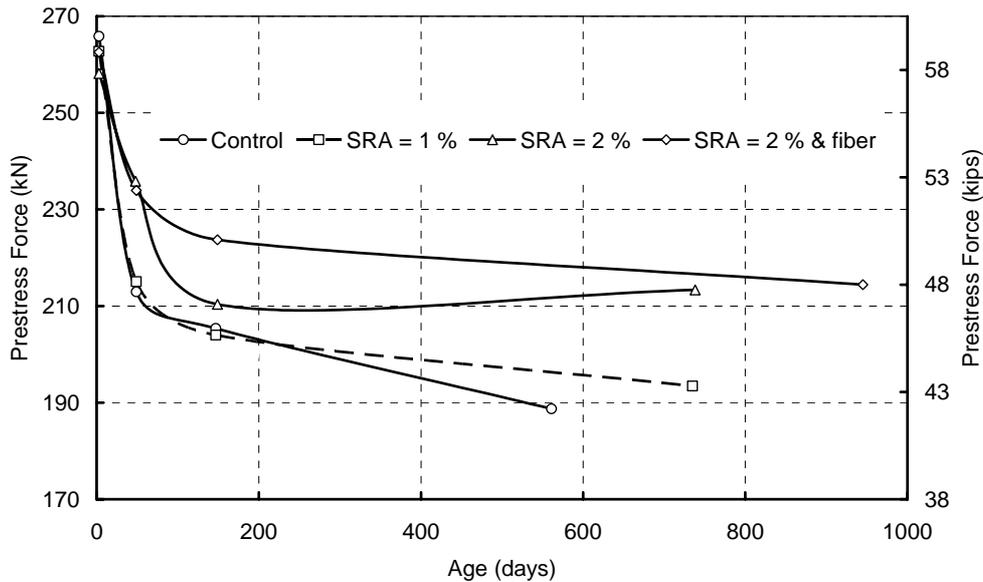
Figure 8: Prestress force in the tested beams

The shapes of the load deflection curves of the fiber reinforced concrete pre-stressed beams (Fig. 4d) relative to the control beams (Fig. 4a) demonstrate the improved global structural response that discrete macro-synthetic fibers add to pre-stressed beams. The benefit can be seen in the ductility after the maximum load is reached. The control beams tested at 561 days maintained the maximum load up to a deflection of 40 mm (1.57 in.), whereas the beam with synthetic macro-fibers tested at 945 days maintained the maximum load up to a deflection of 60 mm (2.36 in.). The effect of the fibers on the pre-stress loss could not be seen from the load versus deflection curves.

Flexural Cracking and Ultimate Loads

The flexural cracking load for the different beams was defined as the point at which a flexural crack formed at the bottom of the beam at the section of maximum bending moment. At this point of loading, the crack can be visually detected with careful examination of cracking at the bottom of the beam. This point also marked a distinct change in the beam stiffness in the load deflection curve and a subsequent deviation from linearity. The flexural cracking load was estimated from the load deflection curve together with visual observation of the beam's cracking. The estimation process was validated through the measurement of concrete strain at the bottom of the beam as shown in

Fig. 6. The measurement of strain at the bottom of the beam was reported by Baran et al. (2005) as the most accurate way to estimate the flexural cracking load in pre-stressed girders. The results of concrete strain at the bottom of the beam with 2% SRA and fibers tested at the age of 945 days are presented in Fig. 6 together with the load deflection curve of the same beam. The strain results suggest that the flexural crack was formed at a load level of around 34 kN (7.6 kips), since the strain gauge measured constant strain with increasing load and

thus the beam experienced a significant change in the concrete strain after cracking (the point circled in Fig. 6). At this point, the crack can be visually observed. The estimated cracking load from the strain gauge matched the load that corresponded to the end of the linear portion in the load deflection curve as shown in Fig. 6, which imparts confidence in the estimate of the cracking load. The cracking load was estimated with an accuracy of ± 0.5 kN (110 lbf) and used in the analysis for the pre-stressing force.
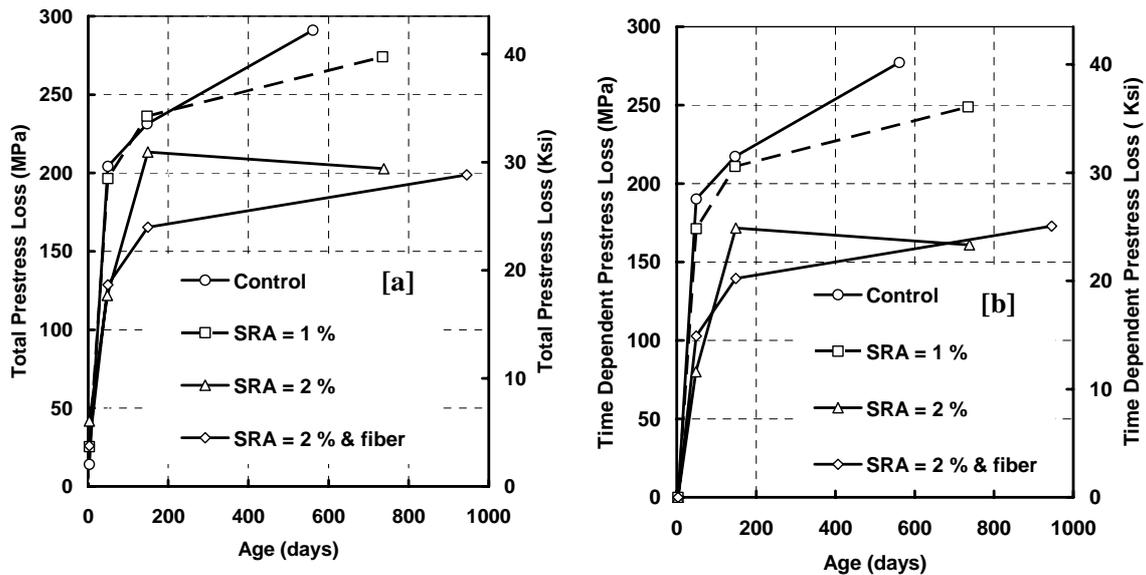
Figure 9: Prestress loss in the beams (a) total loss (b) time dependent loss

The flexural cracking load as estimated in this study is closer to the load at which flexural cracks were formed and visually observed. The initiation of the flexural crack, however, happened at a smaller load, and signs of crack initiation can be seen in the strain results of Fig. 6, where the strain gauge exhibited a slight change in the rate of strain. Similar observation was reported by Shenoy and Frantz (1991), and by Halsey and Miller (1996), where signs of flexural cracking initiation were detected based on the concrete strain data, yet the cracks were not observed at those levels. More importantly, the measured pre-stress force in these studies correlated closely with the predicted prestress force when the visually-observed flexural cracking load

was used for the prediction based on principles of mechanics.

The ultimate load marked the maximum load carrying capacity of the beam. Table 3 presents a summary of the loads corresponding to the flexural crack formation and the ultimate capacity of the beams tested in this study. It also includes the modulus of rupture of the concrete mix at the corresponding age. The results show that the ultimate strength increased with time, which was attributed to the increase of the concrete compressive strength. The flexural cracking load, however, did not follow the same trend and decreased with time due to the time-dependent losses in the pre-stressing force. The flexural cracking load in the

control beam decreased from 38 kN (8.5 kips) at the age of 3 days to 31.5 kN (7.1 kips) at the age of 561 days, despite the increase of concrete compressive strength from 48 MPa to 60.4 MPa (6960 psi to 8760 psi). The beams with 2% of SRA exhibited a change in cracking load from 35 kN (7.9 kips) at the age of 3 days to 34 kN (7.6 kips) at the age of 735 days. The compressive strength of the concrete with 2% SRA increased from 35 MPa to 59.2 MPa (5075 psi to 8585 psi) at the corresponding ages. The rate of change of the cracking

load for control beams was bigger than that for the beams with 2% of SRA. This change in cracking load was mainly attributed to the time-dependent losses of the pre-stressing force. The smaller change in cracking load for the SRA beams was also partly attributed to the increase of concrete strength in time. The variation in concrete strength will be accounted for in the analysis for the time-dependent losses. The results in Table 3 suggest that the pre-stress losses in the control beams were larger than those in the beams with 2% SRA.
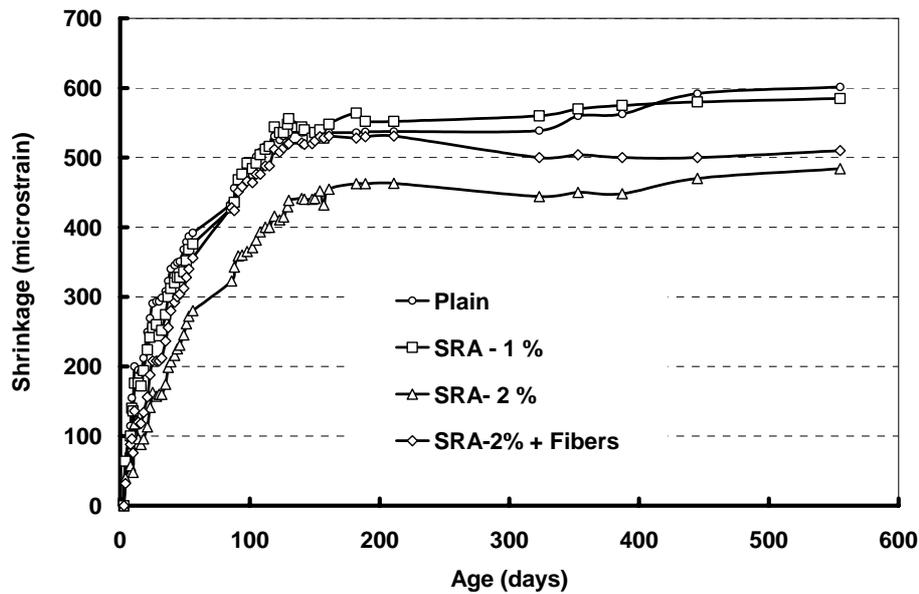
Figure 10: Free shrinkage of the concrete mixtures

Cracking and Failure

Cracking pattern and sequence were carefully monitored and mapped during testing. The formation of the flexural cracks was carefully monitored during the tests by continuous visual inspection of the critical middle section of the bottom of the loaded beams. The load corresponding to the formation of a crack or the extension of an existing crack was documented and marked on the beam. Typically, flexural cracks started at the mid-span and spread out to the shear-span, where the flexural cracks - with increasing load - began to incline as diagonal shear cracks. The beams generally

failed by concrete crushing at the point of maximum bending moment at mid-span. Fig. 7 presents a photograph of a typical cracking pattern of the tested beams.

ANALYSIS AND DISCUSSION OF PRE-STRESS LOSS

The time-dependent losses of steel relaxation and concrete creep and shrinkage are all of significant importance in pre-tensioned girders. However, and because the beams are lightly pre-stressed (each beam has two 15.2 mm (0.6 in.) diameter strands initially

tensioned to 52% of f_{pu}), and a low relaxation steel was used, the pre-stress loss due to strand relaxation was assumed to be negligible. Therefore, the time-dependent losses in the tested beams are primarily driven by creep and shrinkage of the concrete. As mentioned earlier, the flexural cracking load for the tested beams of each set decreased as drying progressed. The biggest change of the cracking load occurred in the control beams and the smallest was measured in the beams that contained 2% of SRA. The decreasing trend of the measured cracking load with time indicates that time-dependent losses of the pre-stressing force have occurred due to creep and shrinkage of the concrete. The variation of the concrete compressive strength, however, necessitates theoretical analysis to estimate the amount of losses. For this purpose, the basic theory of mechanics of pre-stressed concrete was utilized to estimate the pre-stressing force based on the measured cracking load. The flexural cracking load estimated in this study is closer to the load at which flexural crack was formed and not just was initiated as explained before. Thus, the crack at the measured cracking load can be visually seen with careful monitoring. Previous studies showed that the visually observed cracking loads, as opposed to the best estimate of crack initiation, correlate more closely to the pre-stress loss, especially when the basic theory of mechanics is used to predict the effective prestressing force (Halsey and Miller, 1996; Shenoy and Frantz, 1991; Baran et al., 2005).

The effective pre-stress force at the time of testing was back-calculated from the measured cracking load, assuming that the stress at the bottom of the beam is equal to the actual modulus of rupture for the concrete. Using the cross-section properties just before cracking, the effective pre-stressing force can be obtained from the following equation:

$$f_r + \frac{P_{eff}}{A_g} + \frac{P_{eff}\,e}{S_g} = \frac{M_g + M_{applied}}{S_g} = \frac{M_{cr}}{S_g} \qquad (1)$$

where:

f_r = Modulus of rupture;

P_{eff} = effective pre-stress force;

e = eccentricity of the center of gravity of tendons with respect to the center of gravity of the concrete cross-section;

A_g = area of concrete cross-section of the section considered;

S_g = cross-section concrete modulus;

M_g = bending moment due to self-weight of pre-stressed member;

$M_{applied}$ = the moment caused by the measured cracking load.

Table 4 presents the calculated pre-stress forces for all beams at different ages and the prestress force was also plotted against time for all beams in Fig. 8. The pre-stress forces for the SRA beams are greater than those for the control beams and the difference was expressed as a percentage increase of the force at the corresponding ages. The results in Table 4 and Fig. 8 show that the addition of 1% SRA does not significantly affect the pre-stress force relative to the control beam, whereas the addition of 2% SRA to the concrete results in a greater effective pre-stress force at 2 to 3 years by more than 13% relative to the control, which is attributed to the reduction of time-dependent losses. At this concrete age, the majority of drying shrinkage has already occurred.

Based on the pre-stress forces reported in Table 4, the total and time-dependent pre-stress losses were calculated. The total loss was evaluated using the initial pre-stressing force of 270 kN (60.7 kips) as the reference point. The time-dependent loss was evaluated using the force at 3 days as the reference point, since at this age the instantaneous and initial losses had already occurred. The total and TD pre-stress losses with time for all beams are plotted in Fig. 9a - b. The results show that the control beam experienced the largest total loss, while the beams with 2% SRA experienced the smallest total loss, among all beams. The total pre-stress loss was 290.9 MPa (42.2 ksi) at 561 days for control beams; 274.1 (39.7 ksi) at 735 days for the beams with 1% SRA; 202.7 MPa (29.4 ksi) at 735 days for the beams with 2% SRA; and 198.7 MPa (28.8 ksi) at 945 days for beams with 2% SRA and 0.5% fibers. The instantaneous

losses depend on the concrete strength at the time of transfer. As mentioned earlier, the beams with SRA had a lower strength relative to control beams at transfer, and thus, it exhibited larger initial losses which in turn should amplify the total losses. The results in Fig. 9a show the opposite and present a smaller total loss for the SRA beams than the control despite the greater initial losses experienced by the SRA beams. This strongly suggests that the SRA significantly modifies the time-dependent losses.

The TD losses were calculated to eliminate the effect of the variation in the concrete strength at the time of transfer and the associated variation in the initial losses. The TD pre-stress losses for all beams calculated relative to the force at the age of 3 days are presented in Fig. 9b. The results show that the control beam experienced the largest TD pre-stress loss, while the beams with 2% SRA exhibited the smallest loss among all. The TD pre-stress loss in the control beam reached 277 MPa (40.2 ksi) at the age of 561 days, whereas it reached 248.7 MPa (36.1 ksi) at the age of 735 days for the beam with 1% SRA. Unlike the control beams, the beams with 2% SRA experienced a TD pre-stress loss of 160.9 MPa (23.3 ksi) at the age of 735 days and 172.9 MPa (25.1 ksi) at the age of 945 days.

Table 5 presents the percentage decrease (relative to the control beam) of the total and TD losses due to the addition of SRA. The long-term TD pre-stress losses at the age of 735 days were found to be at least 10% and 41.9% less than those of the control beam when SRA was added at 1% and 2% , respectively. The addition of SRA at 2% also reduced the TD pre-stress loss by 37.6 % at the age of 945 days. Similarly, the long-term total loss after 735 days was reduced by 5.8% and 30.3% due to the addition of SRA at 1% and 2%, respectively. The addition of SRA at 2% also reduced the total loss by 31.6% after 945 days of drying. Furthermore, the percentage decrease of the long-term losses for the SRA beams at 735 and 945 days was calculated relative to the pre-stress force of the control beam at the age of 561 days. Therefore, the reported values in Table 5 can be viewed as lower bounds for the effect of SRA on the pre-stress loss reduction. The results indicate that the addition of SRA to the concrete significantly reduced the pre-stress losses due to shrinkage and creep, particularly when added at 2%.

Fig. 10 shows the free shrinkage of the four concrete mixtures measured according to ASTM C157-06 on standard prisms. For each concrete mix, the average shrinkage of 3 specimens was used to plot the curves shown in Fig. 10. The free shrinkage results indicate a significant reduction of the shrinkage when SRA was added to the concrete at 2%. Conversely, the effect of 1% of SRA on the free shrinkage of concrete was nominal. The free shrinkage of the concrete at the age of 555 days was in the order of 500 micro-strains for the concrete with 2% SRA and in the order of 600 micro-strains for the control, which corresponds to 17% reduction of the long-term shrinkage due to the addition of 2% SRA. This difference will be greater in the real beams, since big beams shrink less than the standard free-shrinkage specimens. This is due to the difference in the size and the volume to surface ratio. At this age, the pre-stress forces in the beams with 2% SRA were by more than 13 % greater than those in the control beams (Table 4), and the reduction of the percentage loss was up to 41% (Table 5). Likewise, the pre-stress force in the beams with 1% SRA was only about 3% greater than in the control beam and the percentage loss was up to 10%. Considering adding the effect of SRA on the creep component to that on the shrinkage, one can infer that the results for the pre-stress force and time-dependent losses are generally consistent with the free shrinkage test results.

SUMMARY AND CONCLUSIONS

Structural testing of sixteen large scale pre-stressed beams under center-point loading was conducted to determine whether shrinkage reducing admixtures could reduce the time dependent (TD) losses caused by shrinkage and creep of concrete. The beams were reinforced with 2 seven-wire, 15.2 mm (0.6 in.) in diameter, low relaxation strands of Grade 270. The

strands were pre-tensioned to a nominal stress equal to 52% of the ultimate strength. The SRA was added at different dosage rates; namely 0%, 1% and 2% by weight of cement. Four sets of beams were made and labeled as control beams; beams with 1% SRA; beams with 2% SRA; and beams with 2% SRA and fibers. One beam was tested from each group at each age. Three sets of testing were conducted at the ages of 3, 49 and 148 days. The last set was tested after long drying and conducted at the age of 561 days for control beams, 735 days for the beams with 1% and 2% SRA and 945 days for the beams with 2 % SRA and fibers.

Load deflection curves and flexural cracking load and ultimate capacity of the beams were measured. The cracking load was estimated using the load deflection response together with the measured concrete strain at the bottom of the beam and visual observation of cracking. The cracking load was used to evaluate the effective prestress force at the time of testing based on principles of mechanics, and then the pre-stress loss was calculated. The TD loss was estimated as 277 MPa (40.2 ksi) for control beams at 561 days; 248.7 MPa (36.1 ksi) at 735 days for the beams with 1% SRA; 160.9 MPa (23.3 ksi) at 735 days and 172.9 MPa (25.1 ksi) at 945 days for the beams with 2% SRA.

The test results demonstrate a general trend for the SRA to reduce the total and time-dependent pre-stress losses. The reduction is particularly significant when the SRA is added at 2%. The addition of SRA at 1% and 2% reduced the TD pre-stress loss at the age of 735 days by 10% and 41.9%, respectively. The addition of SRA at 2% also reduced the TD pre-stress loss by 37.6 % after 945 days of drying.

A similar effect of SRA was also found on the total loss despite the lower early strength at transfer. The addition of SRA at 1% and 2% reduced the total losses at the age of 735 days by 5.8% and 30.3%, respectively. The addition of 2% SRA also reduced the total loss at 945 days by 31.6%. The reduction of the total loss would have been even greater should the manufacturer's recommendation of adding SRA have been followed to offset the possible reduction of early strength which influenced the initial losses.

The results obtained in this study including load-deflection behavior, cracking loads, total and time-dependent pre-stress losses demonstrated the significant effect of SRA on pre-tensioned beams. The addition of SRA particularly at 2% significantly reduced the total and time-dependent pre-stress losses, while the effect of SRA at 1% was found nominal.

ACKNOWLEDGEMENTS

REFERENCES

Al-Manaseer, A. and Ristanovic, S. 2004. Predicting drying shrinkage of concrete, *Concrete International,* 26 (8): 79-83.

American Association of State Highway and Transportation Officials (AASHTO). 1998. LRFD Specification for Highway Bridges: Second Edition. Washington, D.C.

American Association of State Highway and Transportation Officials (AASHTO). 1996. Standard Specification for Highway Bridges: Sixteenth Edition. Washington, D.C.

American Concrete Institute (ACI) 209R-92 (Reapproved 1997). 2001. Prediction of creep shrinkage and temperature effects in concrete structures, Farmington Hills, MI.

Baran, E., Shield, C.K. and French, C.E. 2005. A comparison of methods for experimentally determining prestress losses in pretensioned concrete girders, *ACI-SP23*, 161-180.

Bazant, Z. P. and Baweja, S. 1995. Creep and shrinkage prediction model for analysis and design of concrete structures-model B3, RILEM recommendations. *Materials and Structures,* 28: 357-365.

Berke, N.S., Dallaire, M.P., Hicks, M.C. and Kerkar, A. 1997. New developments in shrinkage reducing admixtures, superplasticizers and other chemical admixtures in concrete, *ACI SP-173*: 971-998.

CEB-FIP. 1991. Model Code 1990, Comitè Euro-International Du Beton, Bulletine D' Information No. 203.

Christopher J. Waldron. 2004. Investigation of long-term prestress losses in pretensioned high performance concrete girders, Ph.D. Thesis, Civil Engineering, Virginia Polytechnic Institute and State University, 220.

D'Ambrosia, M., Altoubat, S., Park, C. and Lange, D. 2001. Early age tensile creep and shrinkage of concrete with shrinkage reducing admixtures, Creep, Shrinkage and Durability Mechanics of Concrete and other Quasi-Brittle Materials, Elsevier Science, Ltd., New York.

D'Ambrosia, M. 2002. Early age tensile creep and shrinkage of concrete with shrinkage reducing admixtures, Master Thesis, University of Illinois at Urbana-Champaign, 66.

Folliard, K. J. and Berke, N. S. 1997. Properties of high performance concrete containing shrinkage reducing admixtures. *Cement and Concrete Research,* 27 (9): 1357-1364.

Gardner, N. J. and Zhao, J. W. 1993. Creep and shrinkage revised, *ACI Materials Journal,* 90 (3): 236-246.

Gross, S. P. and Burns, N. H. 1996. Implementation of high strength high performance concrete in two Texas highway overpass structures, *Transportation Research Record*, 2: 179-187.

Halsey, J. T. and Miller, R. 1996. Destructive testing of two forty-year-old prestressed concrete bridge beams, *PCI Journal*, 41 (5): 84-93.

Labia, Y., Saiidi, M.S. and Douglas, B. 1997. Full-scale testing and analysis of 20 –year old pretensioned concrete box girders, *ACI Structural Journal*, Sept-Oct., 94 (5): 471 -482.

Nmai, C.K., Tomita, R., Hondo, F. and Buffenbarger, J. 1998. Shrinkage-reducing admixtures. *Concrete International*, 20 (4): 31-37.

Onyemelukwe, O.U., Issa, P.E.M. and Mills, C.J. 2003. Field measured prestress concrete losses versus design code estimates, *Experimental Mechanics*, June, 43 (2): 201-215.

Pessiki, S., Kaczinski, M. and Wescott, H. H. 1996. Evaluation of effective prestress force in 28-year- old pretressed concrete bridge beams, *PCI Journal*, 41 (6): 78-89.

Precast/Prestressed Concrete Institute (PCI) Committee on Prestress Losses. 1975. Recommendation for estimating prestress losses. *PCI Journal,* 20 (4): 43-75.

Precast/Prestressed Concrete Institute (PCI). 1997. *Bridge Design Manual,* Chicago, IL.

Rabbat, B. G. 1984. 25 year old prestressed concrete bridge girders tested, *PCI Journal*, 29 (1): 177-179.

Shah, S.P., Karaguler, M.E. and Sarigaphuti, M. 1992. Effects of shrinkage reducing admixtures on restrained shrinkage cracking of concrete, *ACI Materials Journal*, 89: 88-90.

Shah, S. P., Weiss, W. J. and Yang, W. 1997. Shrinkage cracking in high performance concrete. *International Symposium on High Performance Concrete,* New Orleans.

Shams, M. K. and Kahn, L. F. 2000. Time-dependent behavior of high-strength concrete: task 3, use of high strength/high performance concrete for precast prestressed concrete bridges in Georgia. Structural Engineering, Mechanics and Materials Research Report No. 00-1, Georgia Institute of Technology, Atlanta GA.

Shenoy, C. V. and Frantz, G. C. 1991. Structural tests of 27-year old prestressed concrete bridge beams, *PCI Journal*, 36 (5): 80-90.

Stallings, J. M., Barnes, R. W. and Eskildsen, S. 2003. Camber and prestress losses in Alabama HPC bridge girders, *PCI Journal*, Sep-Oct., 48 (5): 90-104.

Tadros, M. K., Al-Omaishi, N., Seguirant, S.J. and Gallt, J.G. 2003. Prestress losses in pretensioned high-strength concrete bridge girders, NCHRP Report 496, Transportation Research Board, Washington, D.C.

Yang, Y. and Myers, J. J. 2005. Prestress loss measurements in Missouri's first fully instrumented HPC bridge, *TRB 84th Ann. Meeting*, Jan 9-13, Washington, D. C.